L. Tribouilloy[1], F. Vaillant[1], J.-M. Olive[2], M. Puiggali[2]
[1]EDF R&D, Moret sur Loing 77-818 France
[2]Université de Bordeaux I, 351, cours de la Libération 33405 Talence cedex, France

STRESS CORROSION CRACKING ON COLD-WORKED AUSTENITIC STAINLESS STEELS IN PWR ENVIRONMENT

ABSTRACT

Types 304L and 316L austenitic Stainless Steels (SS) are widely used in PWR environment. These past few years, a limited number of cases of intergranular stress corrosion cracking (IGSCC) have been detected in cold worked areas of non sensitized austenitic stainless steel components. A first study has been initiated at EDF to assess the conditions of the cracking. The main results include cold work thresholds of 240 $HV_{0,1}$ for initiation cracking, and of 310 $HV_{0,1}$ for crack propagation, and propose that a dynamic loading is necessary for SCC. The aim of the present paper is to provide a basis of a crack propagation model by investigating the effect of loading, material and cold-work. In order to try to approach a static loading, a trapezoidal cyclic loading is applied on high cold-worked (by rolling or by tensile loading) materials. It is shown that, for the most severe loading, the rolling cold-worked (RCW) materials undergo TGSCC whereas IGSCC is observed after tensile cold-working (TCW). The ratio of loading R has such a strong impact on the crack growth rate (CGR) that it modifies the mechanism of cracking. Moreover, we notice that CGR increases with the applied K_{max} but this evolution depends on the R value. Therefore, ΔK is chosen to represent the mechanical loading effects on CGRs. Finally, the CGR after a hold time of 1 hour is quite the same than for 3 hours. Additionally, to address the critical issue of the effect of the crack tip strain rate on crack growth rate, Slow Strain Rate Tests (SSTR) are carried out on RCW specimens and provide a first relation which is not consistent to a pure anodic process. This study is going on TCW specimens

Key words: *304L-316L stainless steel, cold-work, SCC, PWR*

INTRODUCTION

Austenitic stainless steels (ASS) are widespread in primary circuits of PWR plants because of their good resistance to general corrosion at elevated temperature. These past few years, a limited number of cases of intergranular stress corrosion cracking (IGSCC) were detected in cold worked areas of non sensitized austenitic stainless steel components. Some SCC tests were conducted in order to determine the threshold values of hardness for SCC occurrence and to highlight the effect of pre-straining on CGR and SCC morphology [1]. The necessary conditions found for SCC to occur were hardness levels (240 $HV_{0,1}$ for initiation and 310 $HV_{0,1}$ for propagation) and a dynamic loading. In this context, this study is conducted on AISI type 304L and 316L stainless steels (SS), to provide a basis of a crack propagation model taking into account the effects of mechanical and material parameters on crack growth rates in PWR environment.

EXPERIMENTAL PROCEDURES

Materials

304L and 316L austenitic stainless steels (SS) tested in this work are provided in two plates, 30 mm thick. The chemical compositions are given in *Table 1*. The plates are solution annealed at 1050°C, then water quenched. The resultant microstructure is characterized by a grain size of 60 μm in 304L SS and 90 μm in 316L SS. According to Schaeffler diagram (Fig. 1), 304L SS contains less than 5 % of residual δ-ferrrite (parallel bands in Fig. 2). As predicted, the 316L SS doesn't contain so much ferrite (Fig. 3).

Table 1. *Chemical compositions of 304L and 316L stainless steels*

	C	S	P	Si	Mn	Ni	Cr	Mo	N	Co	Cu	Ti	Al
RCCM220	<0.03	<0.03	<0.045	<1	<2	<8-12	<17-20				<1.00		
304L	0.026	0.002	0.027	0.52	1.49	9.45	19.23	0.24	0.064	0.07	0.17	<0.005	0.033
RCCM220	<0.03	<0.03	<0.040	<1	<2	>10-14	>16-19	<2,25-2,75	<0,06		<1.00		
316L	0.026	0.004	0.033	0.42	1.81	12.00	17.34	2.57	0.05		0.03		

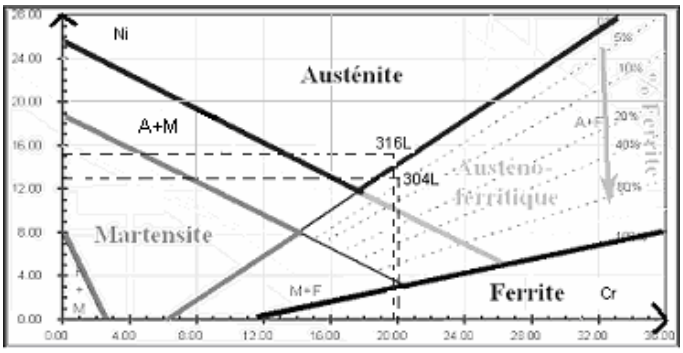

Fig.1. Schaeffler diagram [2]

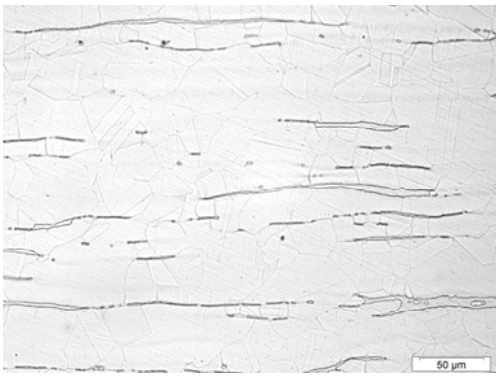

Fig.2. Microstructure at mid thickness on 304L SS

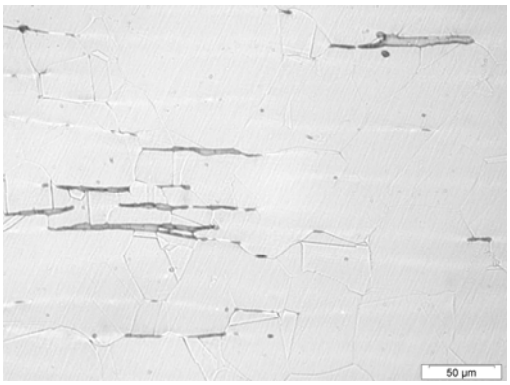

Fig.3. Microstructure at mid thickness on 316L SS

The mechanical properties at room temperature and at 360°C, reported in Table 2, are isotropic.

Table 2. *Mechanical properties of 304L and 316L plates solution annealed*

		$Rp_{0,2}$ (MPa)	Rm (MPa)	A %	Z%	E (MPa)
20°C	Spécification RCCM-M220	>170	>500	>45	-	-
	304L	251	589	60	80	200 000
	316L	255	553	63	72	200 000
360°C	Spécification RCCM-M220	>105				
	304L	157	449	40	72	180 000
	316L	147	445	42	50	189 000

Cold-working and specimens

Two types of cold-working are tested : Tensile Cold-Working (TCW) and Rolling Cold-Working (RCW). In our study, TCW(26%) or TCW(36%) consists in cold drawing the plate up to 26% or 36%, and RCW(30%) or RCW(40%) in rolling up to a thickness reduction of 30% or 40%. After cold working, mechanical properties are not isotropic and 304L stainless steel may be subject to strain-induced martensite transformation [3]. Therefore tensile tests have still to be determined on cold-worked specimens, taking account the loading direction of SCC tests.

CT specimens are machined at mid thickness of the cold-worked plates in order to increase the strain incompatibilities during SCC tests (Fig.4).

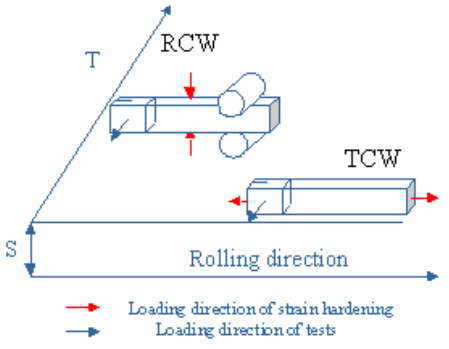

Fig.4. The two types of cold-working

Stress corrosion test procedure

Specimens are ultrasonically cleaned in ethanol and rinsed in distilled water. Tests are carried out in static Hastelloy autoclaves. Specimens are insulated from the autoclave by using zirconia's sleeves to avoid galvanic coupling and to use the DC potential drop technique for crack monitoring. The environment is primary water (1000 ppm B as boric acid, 2 ppm Li as lithium hydroxide) at 360°C. The solution is first de-aerated by evaporating 20% of the initial volume at 125°C in the autoclave, then hydrogen overpressure is introduced (30 cc/kg) and controlled using a Ag/Pd probe. After 100 hours at elevated temperature, the load is applied. The mechanical loadings are the following :

- ✓ Trapezoidal cyclic loading tests (Fig.5) with different parameters to approach a static loading (Fig.6).
- ✓ Constant extension rate tests to obtain a relationship between the crack growth rate and the crack tip strain rate (SSRT).

The fracture surfaces are analysed using scanning electron microscopy (SEM) to confirm the crack morphology and measure the crack growth rate.

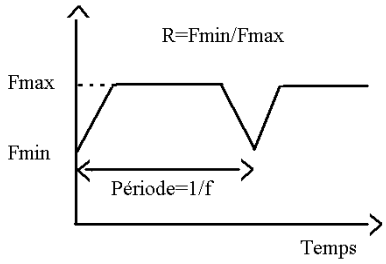

Fig.5. Trapezoidal wave form

Specimen types

304L CT_{15} no pre-strained
304L CT_{15} pre-strained by rolling 40% and 30%
304L CT_{15} pre-strained by traction 36% and 26%
316L CT_{15} pre-strained by traction 36%

Parameters

R	K_{max} (MPa√m)	f (Hz)
0.7	30	$2.9.10^{-4}$
0.8	40	10^{-4}
0.95	50	$2.9.10^{-5}$
1		

Fig.6. Specimens and trapezoidal loading parameters

RESULTS AND DISCUSSION

Effect of cold-working on the propagation mode

Under the most severe mechanical cyclic loading (R=0.7, K_{max}=40MPa√m and f=$2.9.10^{-4}$ Hz), two types of fracture morphology are observed :

- ✓ TGSCC on RCW specimen (except for the finger-like cracks (delaminations) which are purely intergranular and perpendicular to the main crack plane (Fig.7).
- ✓ IGSCC on TCW (26% or 36%) specimen, after a few micrometers of TGSCC (Fig.8).

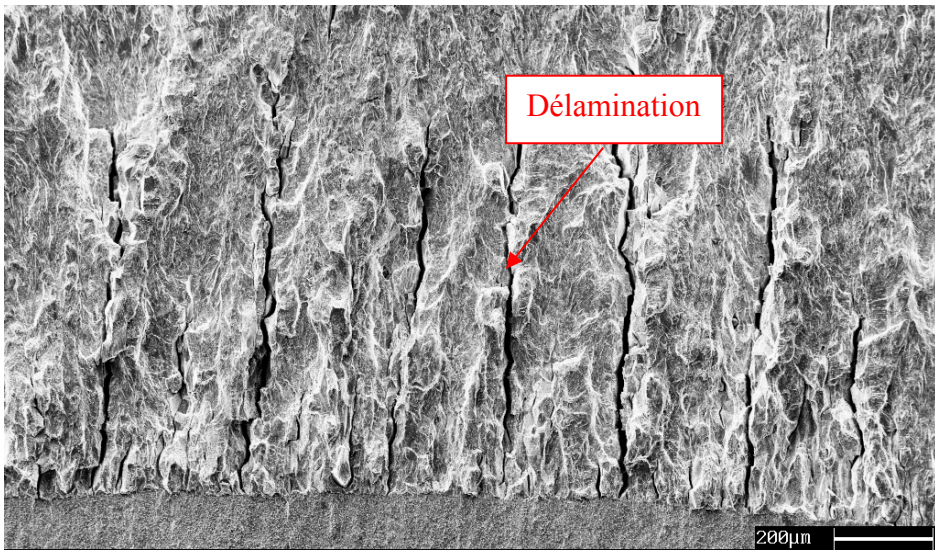

Fig.7. 1368-4E4, RCW (40%) specimen, crosshead speed 2.10^{-7} mm.s^{-1}, 31.2< K_{max} (MPa√m) <56.7

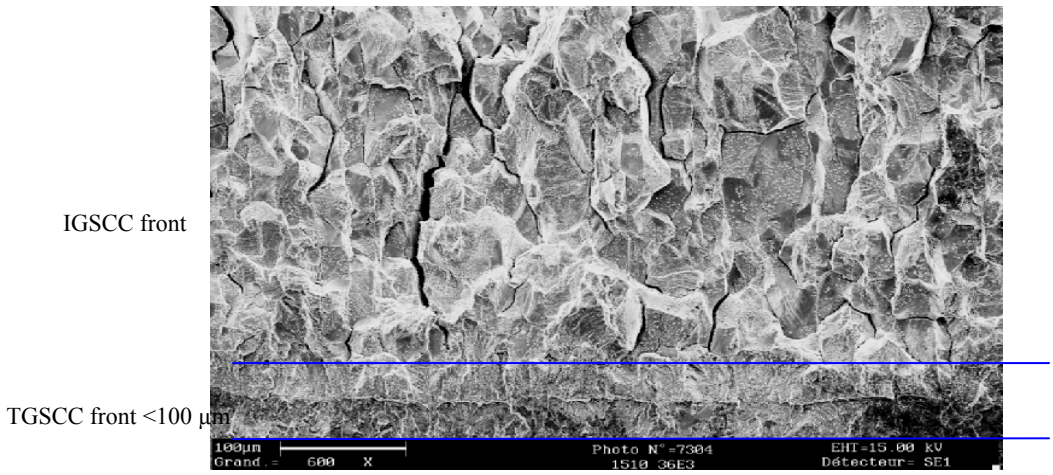

Fig. 8. 1510-36E3 TCW (36%) specimen, trapezoidal loading (R=0.7, f=2.9.10^{-4} Hz, K_{max}=30 MPa√m, 1513 h)

Moreover, we notice that delaminations disappear under the corrosion-fatigue conditions (2.10^{-2} Hz and R=0.6), therefore delaminations are produced by a SCC phenomenon.
Cold-working by tensile is chosen to carry on tests because of two main advantages :

- ✓ the fracture surface is much more regular than for the rolled specimen.
- ✓ the fracture surface is predominantly intergranular (beyond a TGSCC front). Therefore this cold-working seems to favor strain incompatibilities at the grain boundaries.

Effect of trapezoidal cyclic loading parameters on fracture surface

Under a trapezoidal cyclic loading, at R=0.7 and K_{max} = 40 MPa√m, striations are observed both on transgranular cracking in RCW specimen and on intergranular cracking in TCW specimen. The cyclic loading effect on the mechanism of the cracking seems to be important when R≤0.7.
Perpendicular IGSCC secondary cracks cross the TGSCC continuous front in rolled material but they do not overpass the IGSCC front for TCW specimen.
When R>0.7, the fracture surface of RCW specimen changes from TGSCC to IGSCC. However, this change may be due to closest delaminations, when R increases.
Moreover, striations completely disappear both on RCW and TCW specimen.
When R>0.9, only secondary cracks are observed on RCW specimen and no SCC is observed after 2000 hours on TCW specimen.
When K_{max} = 50 MPa√m and R=0.8, we again notice striations on the fracture surface near the faces of the specimen (plane stress). Therefore, the cracking mechanism seems to depend on the ΔK value or K_{max}.

Influence of trapezoidal cyclic loading parameters on the crack growth rates

First, by the crack growth rate decreases with R. The **Fig. 9** shows a strong increase of the CGRs when R reaches 0.7. At R=0.95, the dynamique effect is not sufficient to propagate a crack (excepted IGSCC delaminations). Under a static loading (R=1), no SCC is observed neither on 304L RCW specimen nor on 316L TCW specimen (after 3500 hours and 2000 hours respectively).

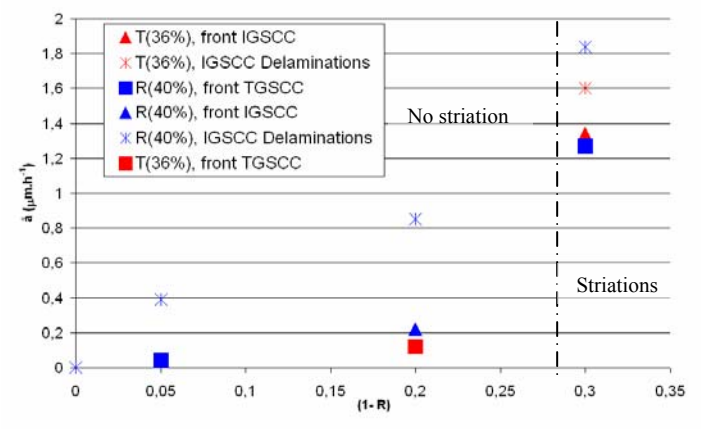

Fig. 9. Influence of R (Trapezoidal loading on 304L specimens, f=2.9.10^{-4} Hz, Kmax =40 MPa√m)

Secondly, the "CGR versus K_{max}" curve (Fig.10) indicates that the threshold for K_{max} is increasing with R. This is the reason why the ΔK parameter seems to be the most appropriated parameter to describe the different results (Fig.11).

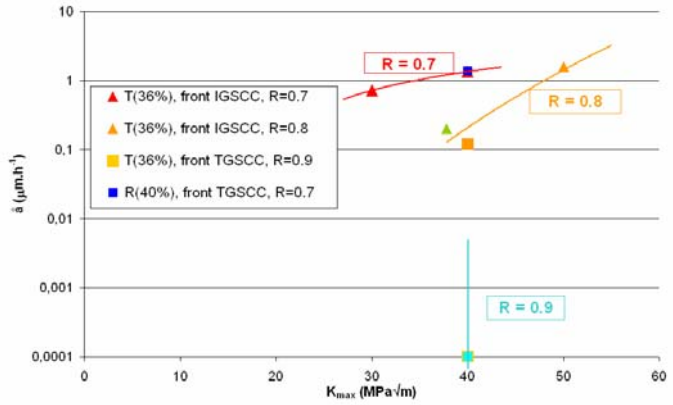

Fig. 10. Influence of K_{max} (Trapezoidal loading on 304L specimens, f=2.9.10^{-4} Hz)

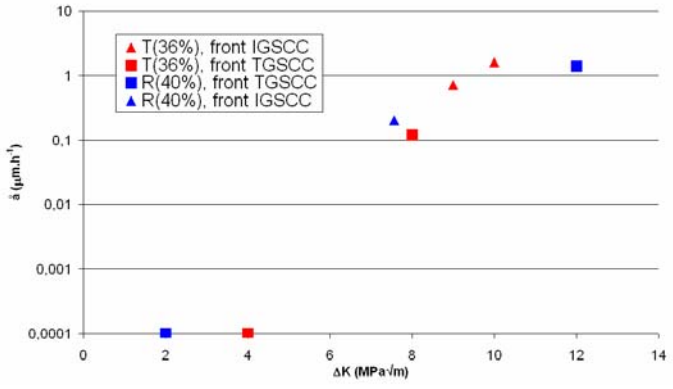

Fig. 11. Influence of □K (Trapezoidal loading on 304L specimens, f=2,9.10^{-4} Hz)

Limited results related to the effect of the hold time on CGR (Fig.12) are available : it seems that the longer the hold time, the lower the CGR. This effect has to be clearly confirmed. Nevertheless, it can be noticed that the crack growth rate with a hold time of 1 hour is quite the same than for 3 hours. The necessary period for propagation from

some tests by the DC potential drop technique, is not taken into account here because we don't know it for each test. An accurate DCPD monitoring could save this problem.

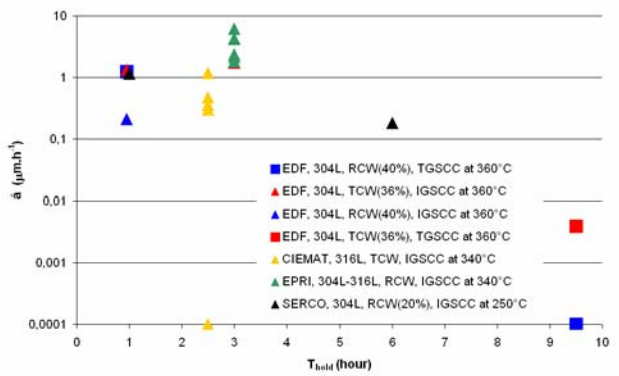

Fig. 12. CGR vs hold time (trapezoidal loading tests, T > 288°C, R = 0.7, 8.10^{-5}< f (Hz) < 3.10^{-4}, 30 < K_{max} (MPa√m)< 40, 700<□$_y$ (MPa)<1035) [4-6]

Influence of the material parameter on CGRs

With the same mechanical conditions, (R=0.7, f=2.9 10^{-4} Hz and K_{max} = 40 MPa√m), TCW 316L specimen did not propagate as well as TCW 304L SS. The reason of this better resistance to SCC is to be investigated in detail.
A level of 26% CW (σ_y=580MPa) do not seem to be sufficient to get SCC propagation on 304L SS.
However, some significant cracking is obtained in a RCW(40%) 316L SS under a static loading by [7] (57 MPa√m, 325°C).
Moreover, when the yield strength is higher than 800 MPa, CGR strongly increases under a trapezoidal cyclic loading (R=0.7, f=10^{-4} Hz and K_{max} between 30 MPa√m and 40 MPa√m) (Fig.13).

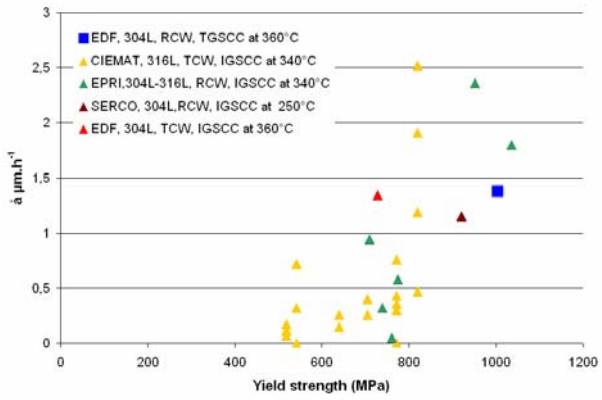

Fig. 13. CGR vs YS (trapezoidal loading tests, T>288°C, R=0.7, 8.10^{-5}< f (Hz) <3.10^{-4} and 30 <Kmax (MPa√m) <40) [4-6]

Influence of the crack tip strain rate

According to Ford [8], the rupture of the passive film and dissolution at the crack tip are the two competitive mechanisms for crack propagation of sensitized SS in BWR

environment : $\dot{a} = K\dot{\varepsilon}_{CT}^{\ n}$. This relationship has yet to be investigated in the case of PWR environment.

Therefore, constant extension rate tests are performed on RCW specimen : crack growth rates are measured on the fracture surfaces and the crack tip strain rates are calculated with finite elements. The TGSCC growth rate clearly depends on crack tip strain rate (Fig.14). Uneven crack fronts make difficult the measurement of crack depths. Despite this problem, a relationship $\dot{a} = 9.10^{7}\,\dot{\varepsilon}_{ct}^{\ 1.29}$ is obtained : the exponent 1.3 is not consistent with a dissolution/repassivation process, estimated at 0.5 by [9] for sensitized SS in high temperature oxygenated water.

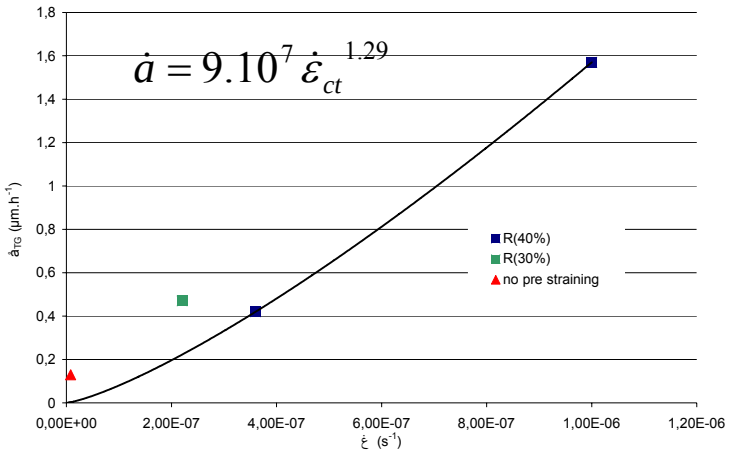

Fig. 14. Relationship between TGCGRs and computed crack tip strain rate

CONCLUSIONS

A previous investigation has defined the required conditions for SCC of 304L : a pre-straining and a dynamic loading leading to $\dot{\varepsilon}_{CT}$. To try to approach a static loading, trapezoidal cyclic loading tests are carried out at very low frequency, on 304L or 316L stainless steels (SS), on tensile cold-worked (TCW) and rolling cold-worked (RCW) specimens.

Firstly, the type of the cold-work modifies the fracture surface morphology of 304L SS : RCW specimen favours TGSCC and TCW favours IGSCC. Therefore the strain path is a major parameter of the fracture mode.

Secondly, the loading ratio R of the trapezoidal cyclic loading can also modify the fracture surface morphology : the TGSCC part decreases when R increases and some striations can appear when R≤0.7. This parameter can change the mechanism of the cracking.

Thirdly, the CGR increases with the level of the loading (K_{max}) and the observed K_{ISCC} increases with R.

Fourthly, no IGSCC is observed with a hold time of 10 hours in a reasonable time (<2000 hours).

Finally, no SCC is obtained on 304L SS after a tensile cold work of 26% specimen, this finding is consistent with a required level of cold-work for cracking.

Taking into account the previous effects of these trapezoidal loading tests, the closest cycle to static loading that leads to propagation cracking is chosen with R=0.8, T_h=57 min and K_{max}=50 MPa√m.
This optimal cyclic loading is currently used for the assessment of the crack initiation stage.
Constant extension rate tests are carried out to test the slip dissolution model of P. Ford on stainless steels in PWR environment. The obtained relationship between the crack growth rate and the crack tip strain rate, $\dot{a} = 9.10^7 \dot{\varepsilon}_{ct}^{1.29}$, is not consistent with a dissolution/repassivation process. Therefore, it doesn't allow to assert this mechanism. This relationship must be investigated on TCW specimens.

REFERENCES

1. T. Couvant, L. Legras, F. Vaillant, J.-M. Boursier, Y. Rouillon, Effect of strain-hardening on stress corrosion cracking of AISI 304L stainless steel in PWR primary environment at 360°C, 2005, 12th International Conference Environmental Degradation of Materials in Nuclear Systems, Snowbird (UT).
2. P. Lacombe, G. Béranger, Structures et diagrammes d'équilibre de diverses nuances d'acier inoxydables, conséquences sur leurs traitements thermiques, 1990, P. Lacombe.
3. Angel, Formation of martensite in austenitic stainless steels, 1954, Journal of iron and Steel Institute, p. 177.
4. D. Tice, N. Platts, K. Rigby, J. Stairmand, H. Fairbrother, Environmentally assisted crack growth of cold worked type 304 stainless steel in PWR environments, 2005, 12th International Conference Environmental Degradation of Materials in Nuclear Systems, Snowbird (UT).
5. T. Shoji, G. Li, J. Kwon, S. Matsushima, Z. Lu, Quantification of yield strength effects on IGSCC in austenitic stainless steels in high temperature water, 2004, 11th Environmental Degradation of Materials in Nuclear Power Systems, Stevenson (W).
6. M. L. Castano, M. S. Garcia, V. De Diego, D. Gomez-Briceno, L. Francia, Effects of hardening on the crack growth rate of austenitic stainless steels in primary PWR conditions, in Fontevraud, (2002).
7. C. Guerre, O. Raquet, E. Herms, M. Le Calvar, G. Turluer, SCC growth behaviour of austenitic stainless steels in PWR primary water conditions, in 12th Environmental Degradation of Materials in Nuclear Power Systems, 2005, Snowbird (UT).
8. P. Ford, Slip dissolution model, Bombannes 1990.
9. P. Ford, P.L. AndresenParkins Symposium on Fundamental Aspects of Stress Corrosion Cracking : Proceeding of a Symposium Sponsored by TMS-ASM-MSD Corrosion and environmental effects committee, TMS, 1992.